

Constrained Minimum-Energy Optimal Control of the Dissipative Bloch Equations

Dionisis Stefanatos^a, Jr-Shin Li^b

^a*Prefecture of Kefalonia, Argostoli, Kefalonia 28100, Greece*

^b*Washington University, St. Louis, MO 63130, USA*

Abstract

In this letter, we apply optimal control theory to design minimum-energy $\pi/2$ and π pulses for the Bloch system in the presence of relaxation with constrained control amplitude. We consider a commonly encountered case in which the transverse relaxation rate is much larger than the longitudinal one so that the latter can be neglected. Using the Pontryagin's Maximum Principle, we derive optimal feedback laws which are characterized by the number of switches, depending on the control bound and the coordinates of the desired final state.

Keywords: Maximum Principle, Bloch Equations

1. Introduction

Optimal control theory [1] has been extensively used recently for the design of pulses that optimize the performance of various Nuclear Magnetic Resonance (NMR) and quantum systems limited by the presence of relaxation [2, 3, 4, 5, 6, 7, 8, 9, 10, 11, 12, 13], the dissipation due to random interactions between the system and its environment. In this letter, we employ tools from optimal control to derive minimum-energy $\pi/2$ and π pulses for a simple NMR system described by the Bloch equations. In particular, we study the case where transverse relaxation dominates the dissipation of the system and the control amplitude is bounded.

The problem of optimal control of the Bloch equations and its closely related corresponding problem for a two-level quantum system have received considerable attention. D' Alessandro and Dahleh [14] considered the problem of minimum-energy optimal control for a two-level quantum system without dissipation. Boscain and Mason [15] examined the time minimal problem for a spin-1/2 particle in a magnetic field neglecting dissipation. Sugny, Kontz and Jauslin [8], Bonnard and Sugny [9] and Bonnard, Chyba and Sugny [10] stud-

Email addresses: dionisis@post.harvard.edu (Dionisis Stefanatos), jsli@seas.wustl.edu (Jr-Shin Li)

ied extensively the problem of time-optimal control for a dissipative two-level quantum system.

In our recent work, we studied the problem of designing minimum-energy $\pi/2$ and π pulses for the Bloch system dominated by the transverse relaxation with unlimited control amplitude [12]. This dissipative system is of great practical importance as it is a very good approximation for many applications of interest. In this article, we extend this previous work to consider the case where the control amplitude is limited, which accounts for realistic limitations of the experimental setup and also makes the problem more interesting from a control theoretic perspective.

In the next section, we formulate the related optimal control problems of such pulse designs. The solutions of these problems are presented in Section 3, which is the main contribution of this article. Then in Section 4, we present some examples to demonstrate our analytical results.

2. Optimal Control of Dissipative Bloch Systems

In a resonant rotating frame, the Bloch equations with the longitudinal relaxation neglected are of the form [16]

$$\dot{z} = u_y x - u_x y \quad (1)$$

$$\dot{x} = -R x - u_y z \quad (2)$$

$$\dot{y} = -R y + u_x z, \quad (3)$$

where $\mathbf{r} = (x, y, z)$ is the magnetization vector, u_x, u_y are the transverse components of the magnetic field and $R > 0$ is the transverse relaxation rate. The above equations constitute a dissipative bilinear control system. By the following change of variables (see Fig. 1(a)) and time rescaling

$$\begin{aligned} a &= \ln r = \ln(\sqrt{x^2 + y^2 + z^2}) \\ \tan \theta &= \sqrt{x^2 + y^2}/z \\ \tan \phi &= y/x \\ t_{new} &= R t_{old}, \end{aligned}$$

we arrive at a new system

$$\dot{a} = -\sin^2 \theta \quad (4)$$

$$\dot{\theta} = u - \sin \theta \cos \theta \quad (5)$$

$$\dot{\phi} = v \cot \theta \quad (6)$$

where $u = (u_x/R) \sin \phi - (u_y/R) \cos \phi$, $v = (u_x/R) \cos \phi + (u_y/R) \sin \phi$ are the normalized components of transverse magnetic field perpendicular and parallel to $\mathbf{r}_\perp = (x, y)$, respectively.

Note that v does not affect the angle θ of the pulse. It just rotates \mathbf{r} around z -axis, resulting in a waste of energy. Thus, optimality requires that $v = 0$ and

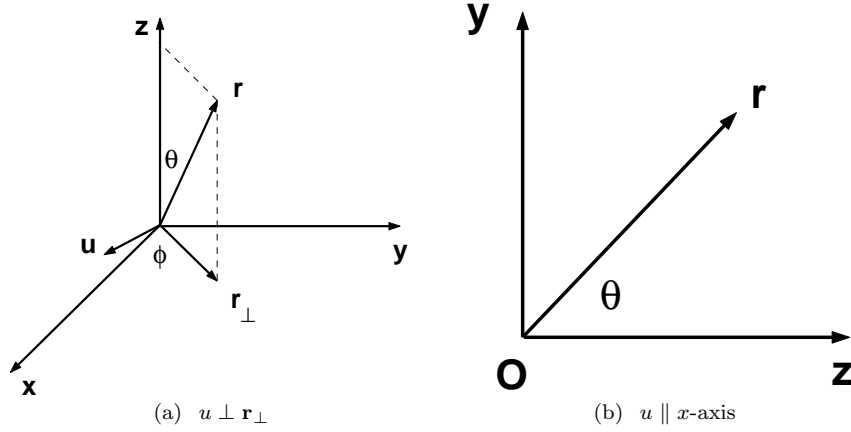


Figure 1: The optimal transverse magnetic field u is perpendicular to \mathbf{r}_\perp and its phase is constant (panel a). Without loss of generality, the experimental setup can be arranged such that $u \parallel x$ -axis. In this case, $\phi = \pi/2$ and \mathbf{r} rotates in yz -plane (panel b). For convenience we display z in the horizontal axis and y in the vertical, so that (r, θ) have the common configuration of polar coordinates on the plane.

hence $\phi = \text{constant}$. If for example we choose u to be parallel to the x -axis, then $\phi = \pi/2$ and \mathbf{r} rotates in yz -plane, see Fig. 1(b). This is the case that we consider in this letter. Equations (4) and (5) are sufficient to describe this rotation.

The optimal control problem that we would like to pursue is formulated as follows. Consider the dynamical system as in (4), (5), starting from $(r(0), \theta(0)) = (1, 0)$ (corresponding to $(a(0), \theta(0)) = (0, 0)$) and for a specified final value $a(\tau) < a(0) = 0$ (equivalent to $r(\tau) < r(0) = 1$), what is the optimal bounded control $u(t)$ with $|u(t)| \leq m \in \mathbb{R}^+$, $0 \leq t \leq \tau$, that accomplishes the transfer between the above starting point and the target point $(a(\tau), \theta(\tau) = \pi/2 \text{ or } \pi)$, while minimizing the energy $E = \int_0^\tau u^2(t)/2 dt$? Note that for the transfers that we study here, it must be $m > 1/2$, otherwise Eq. (5) reaches an equilibrium point $\theta_0 < \pi/2$. Also, the final time τ is unspecified.

3. Derivation of the Optimal Control

The control Hamiltonian for the addressed problem is

$$H = -u^2/2 + \lambda_\theta(u - \sin \theta \cos \theta) - \lambda_a \sin^2 \theta \quad (7)$$

where $\lambda_\theta, \lambda_a$ are the Lagrange multipliers. According to Pontryagin's maximum principle [1], the necessary conditions for optimality of $(u(t), \theta(t), a(t), \lambda_\theta(t), \lambda_a(t))$ are

$$\dot{\lambda}_\theta = -\partial H / \partial \theta = \lambda_\theta \cos 2\theta + \lambda_a \sin 2\theta \quad (8)$$

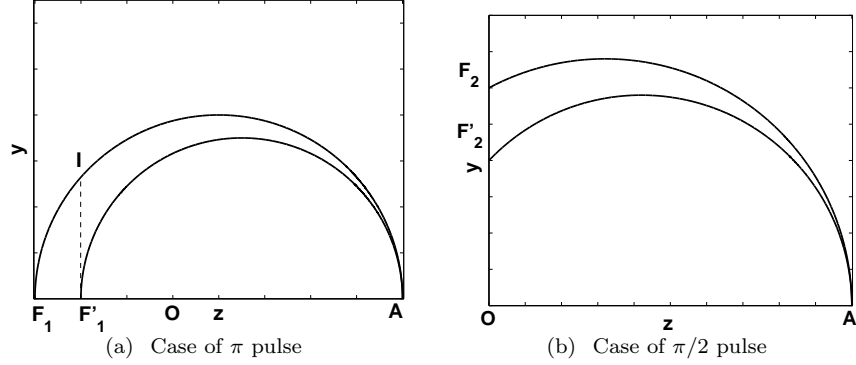


Figure 2: The final point F'_1 can be reached by either following the minimum-energy path AF'_1 , or traveling along AF_1 up to point I and then leaving the system relax to F'_1 (panel a). Analogously, F'_2 can be reached by either following the minimum-energy path AF'_2 , or traveling along AF_2 and then leaving the system relax to F'_2 (panel b).

$$\dot{\lambda}_a = -\partial H/\partial a = 0 \quad (9)$$

$$u = \arg \max_u H(u, \theta, a, \lambda_\theta, \lambda_a) \quad (10)$$

From (9), we immediately know that λ_a is a constant. Additionally, the optimal $(u, \theta, a, \lambda_\theta, \lambda_a)$ satisfies [1]

$$H(u, \theta, a, \lambda_\theta, \lambda_a) = 0, \quad 0 \leq t \leq \tau. \quad (11)$$

Let $E = \min_u \int_0^\tau u^2(t)/2dt$ be the minimum cost corresponding to the optimal solution. Using calculus of variations we find that small changes in the a -coordinate of the final point δa_τ , and small changes in the final time $\delta \tau$, produce the following change in the minimum cost

$$\delta E = \lambda_a(\tau) \delta a_\tau - H(\tau) \delta \tau. \quad (12)$$

Therefore

$$\lambda_a(\tau) = \partial E/\partial a_\tau = \partial E/\partial r_\tau \cdot dr_\tau/da_\tau = \partial E/\partial r_\tau \cdot r_\tau, \quad (13)$$

where $r_\tau = e^{a_\tau}$ is the radius of the final point.

For the transfers that we examine here it is

$$\partial E/\partial r_\tau \geq 0 \quad (14)$$

i.e. the larger the final r , the more energy is needed to quickly rotate the vector before it dissipates. To see this, we refer to Fig. 2. Let E, E' be the minimum energies necessary to reach the final points $F_1(r_\tau, \pi), F'_1(r'_\tau, \pi)$, respectively, with $r'_\tau \leq r_\tau$, see Fig. 2(a). The corresponding minimum-energy paths are AF_1, AF'_1 . An alternative way to reach the point F'_1 is the following: travel along AF_1 up

to the point I , with $z_I = z_{F'_1} = -r'_\tau$, then set $u = 0$ and wait until dissipation eliminates the y -coordinate, see (3). The energy E'' spent for this travel is the portion of E necessary to reach I , so $E'' \leq E$. By the definition of E' it is also $E' \leq E''$, and thus $E' \leq E$. Analogously, let E, E' be the minimum energies necessary to reach the final points $F_2(r_\tau, \pi/2), F'_2(r'_\tau, \pi/2)$, respectively, with $r'_\tau \leq r_\tau$ again, see Fig. 2(b). The corresponding minimum-energy paths are AF_2, AF'_2 . An alternative way to reach the point F'_2 is the following: travel along AF_2 up to the point F_2 , then set $u = 0$ and wait until dissipation brings the system at the point F'_2 , see (3). The energy spent for this travel is the necessary energy to reach F_2 , i.e. E . Then, by definition of E' , it is $E' \leq E$. Thus (14) is true and from (13) we have that $\lambda_a(\tau) \geq 0$. But $\lambda_a = \text{constant}$, so we can set

$$\lambda_a = \kappa^2/2, \quad \kappa \geq 0. \quad (15)$$

Having determined the sign of λ_a , we first examine the case of unbounded control and then we use the developed intuition to study the general case of bounded control.

3.1. Unbounded Control

When the control u is unbounded, then from (10) we conclude that $\partial H/\partial u = 0$. This condition and Eq. (7) yield

$$u = \lambda_\theta. \quad (16)$$

Using (16) and (15), the condition (11) becomes

$$\lambda_\theta^2 - 2\lambda_\theta \sin \theta \cos \theta - \kappa^2 \sin^2 \theta = 0. \quad (17)$$

The optimal u is then given by the following feedback law

$$u(\theta) = \lambda_\theta = \sin \theta (\cos \theta + \sqrt{\cos^2 \theta + \kappa^2}). \quad (18)$$

Note that only the positive solution of the quadratic equation has physical meaning (corresponds to increasing θ) for the transfers that we study here. Using (16) and (18), the validity of (8) can be easily verified. Inserting (18) in (5) we obtain the differential equation for the optimal trajectory

$$\dot{\theta} = \sin \theta \sqrt{\cos^2 \theta + \kappa^2} \quad (19)$$

Eliminating time between (4) and (19) we obtain

$$\frac{da}{d\theta} = -\frac{\sin \theta}{\sqrt{\cos^2 \theta + \kappa^2}}. \quad (20)$$

Integrating the above equation from the starting point $(0, 0)$ to the point $(\ln r, \theta)$, we find the optimal trajectory

$$r(\theta) = \frac{\cos \theta + \sqrt{\cos^2 \theta + \kappa^2}}{1 + \sqrt{1 + \kappa^2}} \quad (21)$$

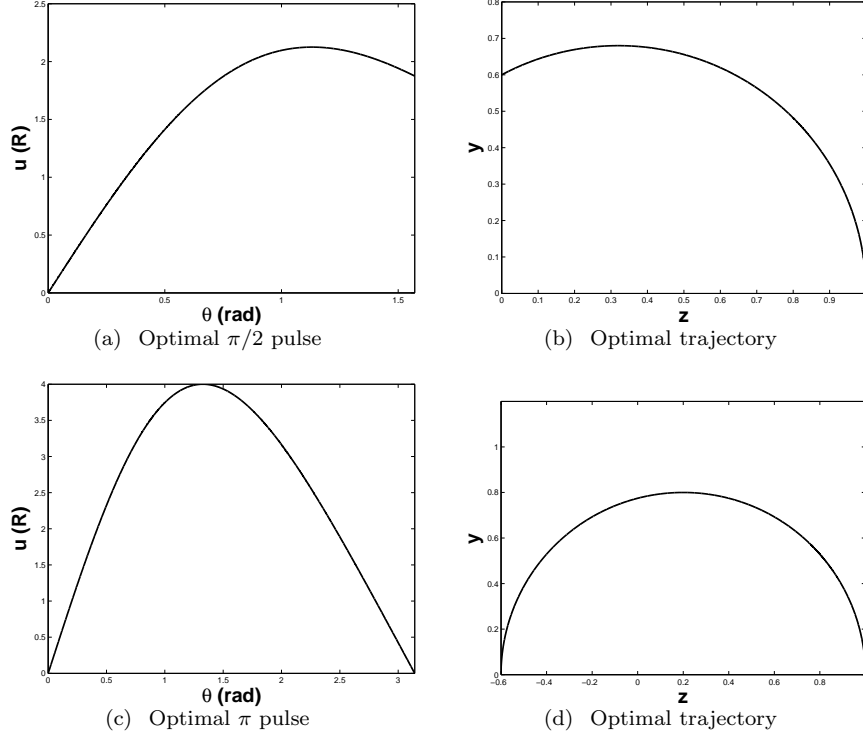


Figure 3: minimum-energy $\pi/2$ (panel a) and π (panel c) pulses for $r_\tau = 0.6$. The corresponding trajectories are also shown (panels b,d).

Setting $\theta_\tau = \pi/2, \pi$ in the above equation, we find the optimal κ for the $\pi/2$ and π pulses, as a function of the radius r_τ of the final point

$$\kappa_{\pi/2} = \frac{2r_\tau}{1-r_\tau^2}, \quad \kappa_\pi = \frac{2\sqrt{r_\tau}}{1-r_\tau} \quad (22)$$

The energy of the optimal pulses is calculated from

$$E = \int_0^\tau \frac{u^2(t)}{2} dt = \int_0^{\theta_\tau} \frac{u^2(\theta)}{2\dot{\theta}(\theta)} d\theta \quad (23)$$

using (18) and (19). The results for $\theta_\tau = \pi/2, \pi$ are

$$E_{\pi/2} = \frac{1}{1-r_\tau^2}, \quad E_\pi = \frac{1+r_\tau}{1-r_\tau} \quad (24)$$

Using (24) in (13), it is easy to verify the validity of (15) with κ given by (22).

In Fig. 3 we plot the optimal $\pi/2$ and π pulses for $r_\tau = 0.6$, as well as the corresponding trajectories. Observe that optimal $u(\theta)$ is small close to $\theta = 0, \pi$

(z -axis), directions that are protected against relaxation, while it is large close to $\theta = \pi/2$ (y -axis), where dissipation is maximized and thus \mathbf{r} must be rotated faster.

3.2. Bounded Control

We now move on to the case where the control is bounded, i.e. $|u| \leq m$, with $m > 1/2$ as pointed out before. The control Hamiltonian (7) is a quadratic form with respect to u that takes its maximum value at $u = \lambda_\theta$, if $|\lambda_\theta| \leq m$, and at the boundary point $u = m$ if $\lambda_\theta > m$. The other boundary point, $u = -m$, corresponds to decreasing θ and has no physical meaning for the transfers that we examine here. Initially, the situation is as in the previous case where the optimality condition $u = \lambda_\theta$ holds and the optimal control is given by (18). Angle θ increases following (19) and u, λ_θ change accordingly. Now suppose that at some point the control reaches the maximum allowable value m . From (18) we see that this happens at the angles that satisfy the equation

$$\sin \theta (\cos \theta + \sqrt{\cos^2 \theta + \kappa^2}) = m, \quad (25)$$

which is equivalent to the following quadratic equation for $\cot \theta$

$$\cot^2 \theta - \frac{2}{m} \cot \theta + 1 - \frac{\kappa^2}{m^2} = 0. \quad (26)$$

If θ_1, θ_2 are the solutions of (26) in $[0, \pi]$, then it is easy to show that for $\theta \in (\theta_1, \theta_2)$ the following inequality holds

$$\sin \theta (\cos \theta + \sqrt{\cos^2 \theta + \kappa^2}) > m. \quad (27)$$

In the interval $\theta \in (\theta_1, \theta_2)$ where the above inequality is true, the relation $u = \lambda_\theta$ gives $u(\theta) > m$ which is not permissible. Thus, the optimal control in this interval is $u(\theta) = m$. From (11) we can find the Lagrange multiplier λ_θ for the same interval, which is

$$\lambda_\theta(\theta) = \frac{m^2 + \kappa^2 \sin^2 \theta}{2(m - \sin \theta \cos \theta)} \quad (28)$$

and $\lambda_\theta(\theta_1) = m$ from (16). This λ_θ satisfies the optimality condition (8) with θ evolving in time according to (5) and $u(\theta) = m$. It is not hard to verify using (27), (28) that $\lambda_\theta > m$ for $\theta \in (\theta_1, \theta_2)$, thus $u(\theta) = m$ is indeed the optimal control in this interval. We call the solutions θ_1, θ_2 of (26), where a change in the optimal control occurs, the *switching angles*. After the second switching, the optimal control is given again by (18), with the same κ as in the initial phase, since $\lambda_a = \kappa^2/2$ is constant along the optimal trajectory.

As explained above, the switching angles determine the optimal feedback law. For $m \geq 1$, Eq. (26) has real solutions for $\kappa \geq \sqrt{m^2 - 1}$. For $1/2 < m < 1$ it has real solutions for every $\kappa \geq 0$. We examine separately these two cases

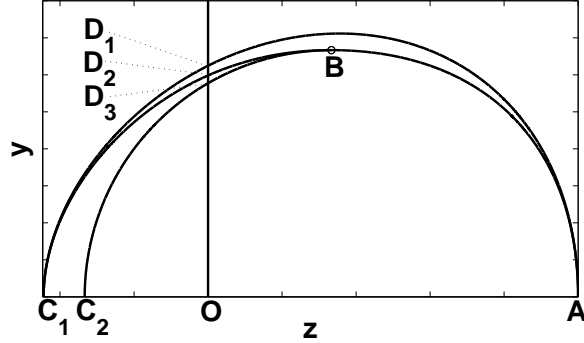


Figure 4: Switching curves AB and BC_1 for the case $m \geq 1$. The outermost curve AC_1 defines the reachable set from the starting point $A(1,0)$ when $u \leq m$. Curve BC_2 is the optimal trajectory for $\kappa = \sqrt{m^2 - 1}$ and $\theta \in [\theta_B, \pi]$. The perpendicular axis $\theta = \pi/2$ crosses the curves AC_1, BC_1, BC_2 at the points D_1, D_2, D_3 , respectively.

3.2.1. $m \geq 1$

For $\kappa > \sqrt{m^2 - 1}$ there are two switching angles, given by

$$\theta_{1,2} = \cot^{-1} \left(\frac{1 \pm \sqrt{\kappa^2 - m^2 + 1}}{m} \right) \quad (29)$$

In this letter the range of the function \cot^{-1} is considered to be $[0, \pi]$, so

$$\cot^{-1}(x) = \pi - \cot^{-1}(-x), \quad x < 0. \quad (30)$$

In the case $\kappa = \sqrt{m^2 - 1}$, the two angles obtain the common value $\theta_B = \cot^{-1}(1/m)$. The angle of the first switching point is in the range $\theta_1 \in [0, \theta_B]$, while that of the second $\theta_2 \in [\theta_B, \pi]$. We find the equation of the first switching curve, i.e. the curve composed by the points (r_1, θ_1) . Before the switching the optimal control is given by (18), so each of the points (r_1, θ_1) belongs to an optimal curve of the form (21), i.e.

$$r_1(\theta_1) = \frac{\cos \theta_1 + \sqrt{\cos^2 \theta_1 + \kappa^2}}{1 + \sqrt{1 + \kappa^2}}. \quad (31)$$

But this κ is related to the switching angle θ_1 through (29), which we re-write as

$$\kappa^2 = (m \cot \theta_1 - 1)^2 + m^2 - 1 \quad (32)$$

since only κ^2 appears in (31). These two equations determine the first switching curve, with the angle θ_1 in the interval $\theta_1 \in [0, \theta_B]$.

After the first switching, the optimal control takes the value $u(\theta) = m$. It maintains this value until the second switching, at angle θ_2 . Between the two switchings the evolution is given by

$$\frac{da}{d\theta} = -\frac{\sin^2 \theta}{m - \sin \theta \cos \theta}, \quad (33)$$

as we derive from (4), (5) with $u = m$. Integrating the above equation from θ_1 to θ_2 we find the radius of the second switching point

$$r_2(\theta_2) = r_1(\theta_1) \sqrt{\frac{2m - \sin 2\theta_1}{2m - \sin 2\theta_2}} \exp \left[-\frac{f(\theta_1, \theta_2)}{\sqrt{4m^2 - 1}} \right] \quad (34)$$

where

$$f(\theta_1, \theta_2) = \cot^{-1} \left(\frac{2m \cot \theta_2 - 1}{\sqrt{4m^2 - 1}} \right) - \cot^{-1} \left(\frac{2m \cot \theta_1 - 1}{\sqrt{4m^2 - 1}} \right) \quad (35)$$

and

$$\theta_2 = \cot^{-1}(2/m - \cot \theta_1). \quad (36)$$

Therefore, to every first switching point (r_1, θ_1) corresponds a second switching point (r_2, θ_2) with angle given by (36) and radius given by (34), (35). These points compose the second switching curve. The two switching curves are plotted in Fig. 4, curves AB and BC_1 . The joint point is $B(r_B, \theta_B)$, where

$$r_B = \frac{\sqrt{m^2 + 1}}{m + 1}. \quad (37)$$

The outermost curve AC_1 corresponds to the trajectory traveled for $u(\theta) = m, \theta \in [0, \pi]$. The equation for this trajectory can be found by setting $(r_1, \theta_1) = (1, 0)$ (starting point A) in (34), (35). It is

$$r_3(\theta_3) = \sqrt{\frac{2m}{2m - \sin 2\theta_3}} \exp \left[-\frac{1}{\sqrt{4m^2 - 1}} \cot^{-1} \left(\frac{2m \cot \theta_3 - 1}{\sqrt{4m^2 - 1}} \right) \right] \quad (38)$$

where we used (r_3, θ_3) to denote a point on the curve and $\theta_3 \in [0, \pi]$. The points between this curve and the horizontal axis define the reachable set from A for a specific control bound m . This curve meets the axes $\theta = \pi, \pi/2$ at the points $C_1(r_{C_1}, \pi), D_1(r_{D_1}, \pi/2)$, where

$$r_{C_1} = \exp \left(-\frac{\pi}{\sqrt{4m^2 - 1}} \right) \quad (39)$$

$$r_{D_1} = \exp \left[-\frac{1}{\sqrt{4m^2 - 1}} \left(\pi - \cot^{-1} \frac{1}{\sqrt{4m^2 - 1}} \right) \right] \quad (40)$$

These are the points with the largest radius along these axes, that can be reached from $A(1, 0)$. Using (31), (32), (34), (35) and (36) we find that the second switching curve BC_1 crosses the axis $\theta = \pi/2$ at the point $D_2(r_{D_2}, \pi/2)$ where

$$r_{D_2} = \frac{\sqrt{m^2 + 2}}{1 + \sqrt{m^2 + 1}} \exp \left[-\frac{1}{\sqrt{4m^2 - 1}} \cot^{-1} \left(\frac{m^2 - 1}{\sqrt{4m^2 - 1}} \right) \right] \quad (41)$$

As we mentioned above, switching takes place only for $\kappa > \sqrt{m^2 - 1}$. For $\kappa \leq \sqrt{m^2 - 1}$ there is no switching and the optimal trajectory is given by (21).

For these values of κ , the optimal trajectory crosses the axis $\theta = \pi, \pi/2$ at points with radius

$$r_\pi = \frac{\sqrt{\kappa^2 + 1} - 1}{\sqrt{\kappa^2 + 1} + 1}, \quad r_{\pi/2} = \frac{\kappa}{\sqrt{\kappa^2 + 1} + 1} \quad (42)$$

respectively, both increasing functions of $\kappa \geq 0$. In Fig. 4 we plot the optimal trajectory without switching for the largest permissible value $\kappa = \sqrt{m^2 - 1}$

$$r_0(\theta_0) = \frac{\cos \theta_0 + \sqrt{\cos^2 \theta_0 + m^2 - 1}}{m + 1} \quad (43)$$

and for $\theta_0 \in [\theta_B, \pi]$. It crosses the axes $\theta = \pi, \pi/2$ at the points $C_2(r_{C_2}, \pi), D_3(r_{D_3}, \pi/2)$ where

$$r_{C_2} = \frac{m - 1}{m + 1}, \quad r_{D_3} = \frac{\sqrt{m^2 - 1}}{m + 1} \quad (44)$$

These are the largest radius points along these axes, that can be reached without switching.

Using the construction shown in Fig. 4 we can find the switching points and the optimal control for any final point of the form $F_1(r_\tau, \pi)$ or $F_2(r_\tau, \pi/2)$. If $F_1 \in C_1C_2$ then the optimal trajectory after the second switching is

$$r(\theta) = r_2(\theta_2) \frac{\cos \theta + \sqrt{\cos^2 \theta + \kappa^2}}{\cos \theta_2 + \sqrt{\cos^2 \theta_2 + \kappa^2}} \quad (45)$$

where

$$\kappa^2 = (1 - m \cot \theta_2)^2 + m^2 - 1 \quad (46)$$

and $S_2(r_2, \theta_2)$ is the second switching point. Eq. (45) is found after integrating (20) from S_2 to F_1 , while (46) holds because $S_2 \in BC_1$, see (29). The final point $F_1(r_\tau, \pi)$ belongs to this curve, so we find

$$r_2(\theta_2) = r_\tau \frac{\cos \theta_2 + \sqrt{\cos^2 \theta_2 + \kappa^2}}{-1 + \sqrt{1 + \kappa^2}} \quad (47)$$

Plotting this curve for $\theta_2 \in [\theta_B, \pi]$, it crosses the second switching curve at the second switching point S_2 . The first switching angle can be found from

$$\theta_1 = \cot^{-1}(2/m - \cot \theta_2). \quad (48)$$

Having determined the two switching angles and the optimal κ , the optimal feedback control is also determined. If $F_1 \in C_2O$ then no switching is necessary and the optimal control is given by (18) with $\kappa = \kappa_\pi$ given by (22).

For $F_2 \in D_1D_2$ there is only one switching. The optimal trajectory after the switching is

$$r(\theta) = r_1(\theta_1) \sqrt{\frac{2m - \sin 2\theta_1}{2m - \sin 2\theta}} \exp \left[-\frac{f(\theta_1, \theta)}{\sqrt{4m^2 - 1}} \right] \quad (49)$$

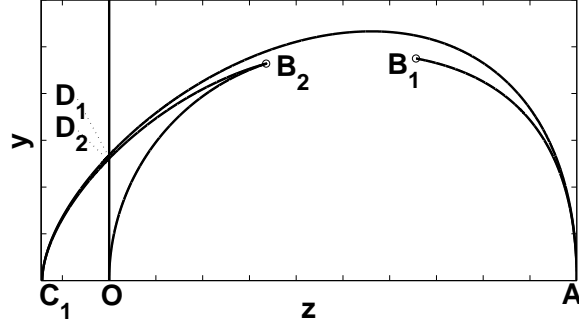


Figure 5: Switching curves AB_1 and B_2C_1 for the case $1/2 < m < 1$. The outermost curve AC_1 defines the reachable set from the starting point $A(1,0)$ when $u \leq m$. Curve B_2O is the optimal trajectory, after the second switching, for the lowest value $\kappa = 0$. The perpendicular axis $\theta = \pi/2$ crosses the curves AC_1, B_2C_1 at the points D_1, D_2 , respectively. Note that for these values of m , switching is inevitable for the transfers that we examine.

The final point $F_2(r_\tau, \pi/2)$ belongs to this curve, so we find

$$r_1(\theta_1) = r_\tau \sqrt{\frac{2m}{2m - \sin 2\theta_1}} \exp \left[\frac{f(\theta_1, \pi/2)}{\sqrt{4m^2 - 1}} \right] \quad (50)$$

Plotting this curve for $\theta_1 \in [0, \theta_B]$, it crosses the first switching curve at the switching point $S_1(r_1, \theta_1)$, so we find the switching angle and the corresponding optimal κ . If $F_2 \in D_2D_3$ then there are two switchings and the situation is similar to the one previously described, with

$$r_2(\theta_2) = r_\tau \frac{\cos \theta_2 + \sqrt{\cos^2 \theta_2 + \kappa^2}}{\kappa} \quad (51)$$

instead of (47), since $\theta = \pi/2$ at the final point. If $F_2 \in D_3O$ then no switching is necessary; the optimal control is given by (18) with $\kappa = \kappa_{\pi/2}$ given by (22).

3.2.2. $1/2 < m < 1$

For this case the two switching curves are described by the same equations as before but now there is no common point but a gap between them, due to the fact that the two roots of (26) are distinct for all $\kappa \geq 0$, see Fig 5. The range for the switching angles is $\theta_1 \in [0, \theta_{B_1}]$, $\theta_2 \in [\theta_{B_2}, \pi]$ where

$$\theta_{B_1} = \cot^{-1} \left(\frac{1 + \sqrt{1 - m^2}}{m} \right) \quad (52)$$

$$\theta_{B_2} = \cot^{-1} \left(\frac{1 - \sqrt{1 - m^2}}{m} \right) \quad (53)$$

The switching points B_1, B_2 correspond to the case $\kappa = 0$ and their radius is

$$r_{B_1} = \sqrt{\frac{1 + \sqrt{1 - m^2}}{2}} \quad (54)$$

$$r_{B_2} = r_{B_1} \times \exp \left[-\frac{1}{\sqrt{4m^2 - 1}} \cot^{-1} \left(\frac{2m^2 - 1}{\sqrt{4m^2 - 1}\sqrt{1 - m^2}} \right) \right] \quad (55)$$

For the lowest value $\kappa = 0$ we plot the optimal curve after the second switching. It is

$$r_0(\theta_0) = r_{B_2} \frac{\cos \theta_0}{\cos \theta_{B_2}} \quad (56)$$

This curve meets the axis $\theta = \pi/2$ at the origin O . Points C_1, D_1, D_2 are defined as before and their coordinates are the same. The situation is as depicted in Fig. 5. Observe that for $1/2 < m < 1$, switching is inevitable for the transfers that we examine; since the control is more restricted than the previous case, the boundary value has to be used to achieve the desired transfers. Any final point of the form $F_1(r_\tau, \pi)$ belongs to C_1O and there are two switchings in the corresponding optimal trajectory. The same happens for $F_2(r_\tau, \pi/2) \in D_2O$, while for $F_2 \in D_1D_2$ there is only one switching.

3.2.3. Summary of the results

We summarize the above results

- $m \geq 1$
 1. $\theta = \pi$
 - (a) $r_{C_2} < r_\tau \leq r_{C_1}$, two switchings
 - (b) $r_\tau \leq r_{C_2}$, no switching
 2. $\theta = \pi/2$
 - (a) $r_{D_2} < r_\tau \leq r_{D_1}$, one switching
 - (b) $r_{D_3} < r_\tau \leq r_{D_2}$, two switchings
 - (c) $r_\tau \leq r_{D_3}$, no switching
- $1/2 < m < 1$
 1. $\theta = \pi$
 - (a) $r_\tau \leq r_{C_1}$, two switchings
 2. $\theta = \pi/2$
 - (a) $r_{D_2} < r_\tau \leq r_{D_1}$, one switching
 - (b) $r_\tau \leq r_{D_2}$, two switchings

If θ_1, θ_2 are the switching angles then the optimal control for $\theta \in (\theta_1, \theta_2)$ is

$$u(\theta) = m \quad (57)$$

while outside this interval is

$$u(\theta) = \sin \theta (\cos \theta + \sqrt{\cos^2 \theta + \kappa^2}) \quad (58)$$

where

$$\kappa = \sqrt{(m \cot \theta_1 - 1)^2 + m^2 - 1} = \sqrt{(1 - m \cot \theta_2)^2 + m^2 - 1}. \quad (59)$$

The switching angles are calculated as described above and are related through

$$\cot \theta_1 + \cot \theta_2 = 2/m. \quad (60)$$

4. Examples

Here we present some examples using specific values for the upper bound m and the coordinates (r_τ, θ_τ) of the final point. We start with the case $m = 2, r_\tau = 0.39, \theta_\tau = \pi$. Using the results of the previous section, it is not hard to see that the optimal trajectory contains two switching points. Plotting Eq. (47) we find that it crosses the second switching curve at the switching point S_2 with angle $\theta_2 = 1.7766$ rad. The first switching angle is found from (60) to be $\theta_1 = 0.6912$ rad. The optimal control is given by (57), (58) with $\kappa = 2.2382$, as it is determined from (59). In Fig. 6(a), 6(b) we plot the optimal pulse and the corresponding optimal trajectory. The two switching points S_1, S_2 are also shown.

For the next example we use the values $m = 2, r_\tau = 0.61, \theta_\tau = \pi/2$. In this case, the optimal trajectory contains only one switching point. Plotting Eq. (50) we find that it crosses the first switching curve at the switching point S_1 with angle $\theta_1 = 0.6124$ rad. The optimal control is given by (58) with $\kappa = 2.5322$ for $\theta \in [0, \theta_1]$ and by (57) for $\theta \in (\theta_1, \pi/2]$. In Fig. 6(c), 6(d) we plot the optimal control and the corresponding optimal trajectory, with the one switching point S_1 .

The last case that we consider is $m = 0.95, r_\tau = 0.2, \theta_\tau = \pi/2$. The optimal trajectory contains two switching points. Plotting Eq. (51) we find that it crosses the second switching curve at the switching point S_2 with angle $\theta_2 = 1.1456$ rad. The first switching angle is found from (60) to be $\theta_1 = 0.5442$ rad. The optimal control is given by (57), (58) with $\kappa = 0.4766$, as it is determined from (59). In Fig. 6(e), 6(f) we plot the optimal pulse and the corresponding optimal trajectory. The two switching points S_1, S_2 are also shown.

5. Conclusion

To conclude, in this letter we calculated minimum-energy $\pi/2$ and π pulses for Bloch equations in the case where transverse relaxation dominates and the control amplitude is bounded, using optimal control theory. This work is expected to find applications in NMR Spectroscopy, Magnetic Resonance Imaging (MRI) and Quantum Information Processing, serving as a reference for numerical studies of more complicated and realistic situations that incorporate for example longitudinal relaxation and magnetic field inhomogeneity.

References

- [1] L.S. Pontryagin, V.G. Boltyanskii, R.V. Gamkrelidze, E.F. Mishchenko, The Mathematical Theory of Optimal Processes, Interscience Publishers, New York, 1962.
- [2] N. Khaneja, T. Reiss, B. Luy, S. J. Glasser, Optimal control of spin dynamics in the presence of relaxation, J. Magn. Reson. 162 (2003) 311-319.

- [3] N. Khaneja, B. Luy, S. J. Glaser, Boundary of quantum evolution under decoherence, *P. Natl. Acad. Sci. USA* 100 (2003) 13162-13166.
- [4] N. Khaneja, J.-S. Li, C. Kehlet, B. Luy, S. J. Glaser, Broadband relaxation-optimized polarization transfer in magnetic resonance, *P. Natl. Acad. Sci. USA* 101 (2004) 14742-14747.
- [5] D. P. Frueh, T. Ito, J.-S. Li, G. Wagner, S. J. Glaser, N. Khaneja, Sensitivity enhancement in NMR of macromolecules by application of optimal control theory, *J. Biomol. NMR* 32 (2005) 23-30.
- [6] D. Stefanatos, N. Khaneja, S. J. Glaser, Optimal control of coupled spins in the presence of longitudinal and transverse relaxation, *Phys. Rev. A* 69 (2004) 022319.
- [7] D. Stefanatos, S. J. Glaser, N. Khaneja, Relaxation-optimized transfer of spin order in Ising spin chains, *Phys. Rev. A* 72 (2005) 062320.
- [8] D. Sugny, C. Kontz, H. R. Jauslin, Time-optimal control of a two-level dissipative quantum system, *Phys. Rev. A* 76 (2007) 023419.
- [9] B. Bonnard, D. Sugny, Time-minimal control of dissipative two-level quantum systems: the integrable case, *SIAM J. Control Optim.* 48 (3) (2009) 1289-1308.
- [10] B. Bonnard, M. Chyba, D. Sugny, Time-minimal control of dissipative two-level quantum systems: the generic case, *IEEE T. Automat. Contr.* to appear.
- [11] L.C. Wang, X.L. Huang, X.X. Yi, Effect of feedback on the control of a two-level dissipative quantum system, *Phys. Rev. A* 78 (2008) 052112.
- [12] D. Stefanatos, Optimal design of minimum-energy pulses for Bloch equations in the case of dominant transverse relaxation, *Phys. Rev. A* 80 (2009) 045401.
- [13] J.-S. Li, J. Ruths, D. Stefanatos, A pseudospectral method for optimal control of open quantum systems, *J. Chem. Phys.* 131 (2009) 164110.
- [14] D. D' Alessandro, M. Dahleh, Optimal control of two-level quantum systems, *IEEE T. Automat. Contr.* 46 (6) (2001) 866-876.
- [15] U. Boscain, P. Mason, Time minimal trajectories for a spin-1/2 particle in a magnetic field, *J. Math. Phys.* 47 (2006) 062101.
- [16] R. R. Ernst, G. Bodenhausen, A. Wokaun, *Principles of Nuclear Magnetic Resonance in One and Two Dimensions*, Clarendon Press, Oxford, 1987.

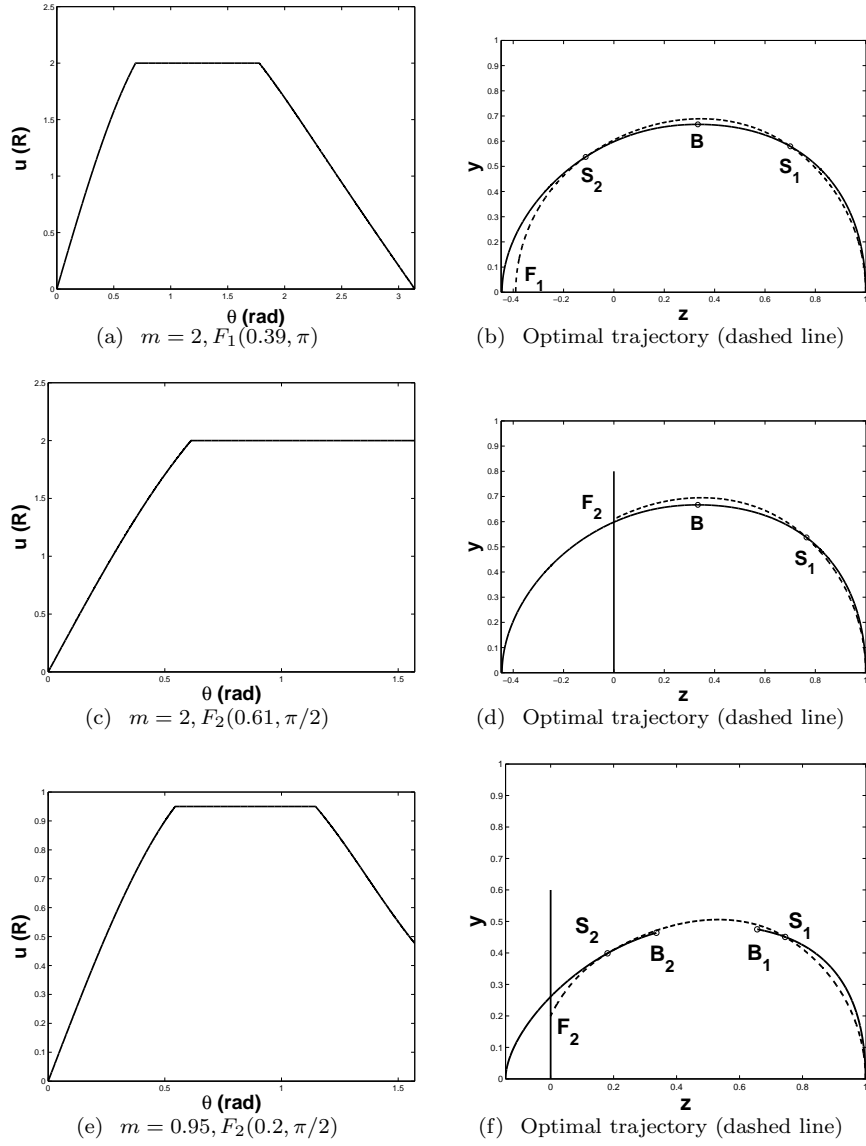


Figure 6: minimum-energy pulses (a, c, e) and corresponding optimal trajectories (b, d, f) for various values of the control upper bound m and the coordinates (r_τ, θ_τ) of the final point. The switching curves and points are also shown.